

Title	Study on residual OH content in low-temperature Si oxide films after in situ post-deposition heating (PDH)
Author(s)	Horita, Susumu; Pu, Di
Citation	Japanese Journal of Applied Physics, 63(01SP12): 1-9
Issue Date	2023-12-20
Type	Journal Article
Text version	publisher
URL	http://hdl.handle.net/10119/18795
Rights	Copyright (c) 2023 Authors. Susumu Horita, Di Pu. Japanese Journal of Applied Physics 63, 01SP12 (2024). This is an Open Access article distributed under the terms of Creative Commons Licence CC-BY [https://creativecommons.org/licenses/by/4.0/]. Original publication is available on IOP Science via https://doi.org/10.35848/1347-4065/acf477 .
Description	



Study on residual OH content in low-temperature Si oxide films after in situ post-deposition heating (PDH)

Susumu Horita* and Di Pu

Japan Advanced Institute of Science & Technology, 1-1 Asahidai, Ishikawa, 923-1292, Japan

*E-mail: horita@jaist.ac.jp

Received July 17, 2023; revised August 20, 2023; accepted August 27, 2023; published online December 20, 2023

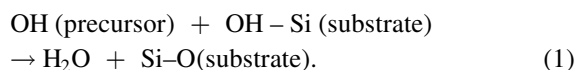
We investigated the post-deposition heating (PDH) effect on OH content in SiO_x films deposited by atmospheric-pressure CVD using a deposition source of silicone oil (SO) with O₃ and TCE vapor at a temperature T_d of 180 °C–250 °C. The PDH is performed in situ for 5 min in the deposition chamber just after film deposition without any supply of SO, where the heating temperature is the same as T_d . The OH content in the films deposited normally decreases with increasing T_d . In contrast, those with PDH decrease with decreasing T_d from 220 °C, and, at $T_d = 190$ °C, a minimum OH content can be obtained. This means that lower OH content remains at a lower deposition temperature. The PDH effect on OH reduction can be explained by easily reconstructible structure of SiO_x films deposited at low temperature. Furthermore, we discuss the mechanism of the PDH effect from other points of view. © 2023 The Author(s). Published on behalf of The Japan Society of Applied Physics by IOP Publishing Ltd

1. Introduction

Low-temperature deposition of silicon oxide (SiO_x) films is required for the fabrication of not only thin-film transistors on non-heat-resistant substrates¹ but also interlayer dielectrics in size-minimizing ICs to suppress the disconnection of the interconnect metal, the redistribution of the dopant, and defect generation in the fabricated underlayer.² For low-temperature deposition, plasma-enhanced CVD (PECVD) has been widely used in practice,^{1,3–6} which requires an expensive system consisting of vacuum equipment and high power supply. In addition, tetraethylorthosilicate [TEOS; Si(OC₂H₅)₄] vapor is commonly used as a deposition gas source.^{3–5} On the other hand, we previously reported on the low-temperature deposition of SiO_x films using silicone oil {SO: dimethylpoly-siloxane (CH₃)₃SiO[(CH₃)₂SiO]₁₀Si(CH₃)₃} vapor as a deposition source and ozone (O₃) gas at temperatures of 200 °C–350 °C at atmospheric pressure without vacuum or pumping systems.^{7,8} SO has advantages over TEOS; the price per unit volume of SO is lower than that of TEOS by about one order, and SO is not only markedly thermally stable, but also a safe material, whereas TEOS is toxic especially to the human eye and throat.⁹

In addition, in order to increase the rate (less than 5 nm min⁻¹) of SiO_x film deposition, by changing SO to decamethylcyclopenta-siloxane, C₁₀H₃₀O₅Si₅, we have reported that adding some amount of trichloroethylene (C₂HCl₃; TCE) vapor markedly increases the deposition rate to more than three times that without TCE during deposition in combination with SO and O₃ at deposition temperatures lower than 200 °C.¹⁰ Furthermore, when using TCE, the OH content in the deposited SiO_x films is much reduced by nearly half of that without it.^{11,12}

This increase in the deposition rate and reduction of OH content are caused by TCE-enhanced dehydration reaction between silanols of the precursors and OH bonds terminated at the surface of the substrate or deposited film, i.e.,



TCE may be decomposed into H and C among others due to the highly reactive O₃, and hydrochloric acid can be formed. Acid added into an organic chemical solution is well known as a catalyst to enhance the dehydration reaction in an organic chemical solution, e.g. the so-called Fischer esterification reaction.¹³

However, using TCE for the SiO_x film deposition with SO + O₃, the deposited films still contain a large number of OH bonds, which have been reported to lead to the serious problems of high leakage current and low breakdown voltage.^{8,14–16} Generally, low-temperature SiO_x films prepared by CVD methods with organic silicon sources, such as TEOS, are more likely to contain a large number of OH bonds when no special treatment is carried out, e.g. post-deposition annealing. In fact, it has already been reported that annealing with higher temperature of more than 400 °C makes residual OH bonds vanish from the deposited film and it improves the electrical properties, e.g. lower leakage current and higher breakdown voltage.^{8,17,18} However, high-temperature annealing may lose some effectiveness of the low-temperature deposition process. Therefore, in order to reduce the number of residual OH bonds before removing a deposited film from the deposition chamber, we treated a deposited SiO_x film by in-site post-deposition heating (PDH) and compared the OH content with that of a non-PDH(NPDH)-treated film. In this paper, having reported some results in the previous conference of EM-NANO 2023,¹⁹ we will provide many more results with respect to the PDH process and deeply discuss them. Finally, we suggest an effective technique to produce a lower-temperature deposited SiO_x film with lower OH content.

2. Experimental

Figure 1(a) shows a schematic diagram of the deposition system used in this study. The system has a vertical reactor for atmospheric-pressure (AP) CVD. The details are mentioned in a previous paper.¹⁰ Before setting n-type (111)Si substrates on a stainless-steel holder, they were chemically cleaned in a hot



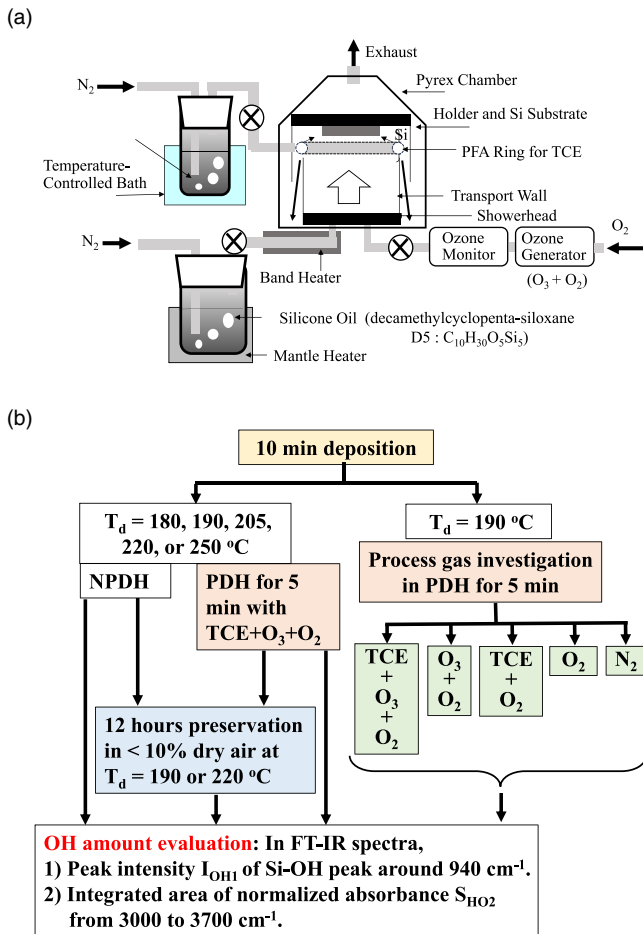


Fig. 1. (a) Schematic diagram of the deposition APCVD system used in this study. Deposition chamber and sample holder are made of Pyrex glass and stainless steel, respectively. (b) PDH process flow. Left- and right-hand sides show the normal PDH process and the PDH processes with various process gases, respectively. NPDPH is an abbreviation of no post-deposition heating.

acid solution and dipped in a dilute HF solution to remove Si oxide. The SO used was decamethylcyclopenta-siloxane ($C_{10}H_{30}O_5Si_5$) heated to $50\text{ }^\circ\text{C}$ using a mantle heater, and its vapor was generated by bubbling with N_2 gas. The flow rate of N_2 gas for the SO vapor, $F_{N_2}(\text{SO})$, was 0.2 lmin (liters per minute at $20\text{ }^\circ\text{C}$). O_3 was generated using a silent electric discharge from 99.9995% O_2 gas at a flow rate of 0.50 lmin and the O_3 concentration was $\sim 150\text{ g m}^{-3}$. The $O_3 + O_2$ mixed gas was introduced into the reaction chamber from the bottom. The TCE vapor was generated by bubbling $20\text{ }^\circ\text{C}$ TEC solution with 0.1 lmin N_2 gas, and the mixed gas of TCE vapor + N_2 gas was introduced into a PFA tube with a $1/4$ inch diameter. The mixed gas was blown onto the Si substrates directly through many $\sim 2\text{ mm-}\phi$ holes made in a PFA tube ring with a diameter of $\sim 110\text{ mm}$. The distance between the ring and the sample holder was $\sim 10\text{ mm}$. SiO_x films were deposited for 10 min at a deposition temperature T_d of $180\text{ }^\circ\text{C}$ – $250\text{ }^\circ\text{C}$. After the deposition, the heating of the sample holder was stopped immediately, and then for the same samples, the supply of SO vapor, TCE vapor and $O_3 + O_2$ gases was stopped and we immediately flowed pure N_2 gas at $\sim 2\text{ lmin}$ onto the sample holder. Soon after the holder was cooled down to $120\text{ }^\circ\text{C}$ from the T_d , the deposited samples were removed from the deposition chamber. This is called the non-post-deposition-heating

(NPDH) process. The other samples, just after the deposition, were heated in situ for 5 min at the same T_d of $180\text{ }^\circ\text{C}$ – $250\text{ }^\circ\text{C}$ without any supply of SO vapor, as shown in the left-hand side of Fig. 1(b). This is the so-called PDH. The gas used for the PDH process was mainly a mixed gas of TCE(+ N_2) + $O_3 + O_2$ or deposition reactant gas without SO vapor. After taking out some samples treated by PDH at $190\text{ }^\circ\text{C}$ or $220\text{ }^\circ\text{C}$, they were preserved in dry air with humidity of less than 10% for 12 h at RT. For comparison, some NPDH samples at $190\text{ }^\circ\text{C}$ or $220\text{ }^\circ\text{C}$ were also preserved. The preservation was done to investigate the PDH effect on the suppression of increase in OH content. Many researchers have already reported that OH content in low-temperature deposition SiO_x films increases during preservation in air mainly due to moisture adsorption on the film surface from the preservation atmosphere.^{4,20,21} Furthermore, gas of the PDH process was changed to $O_3 + O_2$, TCE + O_2 , O_2 or N_2 to investigate the influence of the process gas on OH content in the deposited films, as shown in the right-hand side of Fig. 1(b). For simplification, the name of each PDH process with a different gas combination is abbreviated to P_i , as shown in Table I including the NPDH process, where the subscript i is an integer corresponding to used gaseous species. For example, PDH processes with gases of TCE + $O_3 + O_2$ and $O_3 + O_2$ are labeled as P_1 and P_2 , respectively.

The thicknesses d and refractive indexes n of the deposited films were measured by ellipsometry using four wavelengths of $450, 525, 595,$ and 660 nm from four LEDs (Model FS-1, Film Sense LLC). The molecular structures of the films were analyzed from Fourier transform IR spectroscopy (FT-IR) spectra with a resolution of 4 cm^{-1} and the acquired spectra were averaged with 10 scans. The measured FT-IR spectra were normalized by the highest peak of the Si–O–Si unsymmetric stretching (TO_3) vibration mode around 1065 cm^{-1} , as shown later in Fig. 3(a).^{22–24} In order to improve the signal-to-noise ratio, the measured spectra were computed by two runs of a five-point moving average with a parabolic smoothing function. In addition, we took the 1st derivative of the averaged spectra by using the Savitzky–Golay numerical algorithm with the 2nd-order polynomial at 20 points to estimate the width of the TO_3 mode peak instead of the FWHM.²⁵ The difference in wavenumber k between the 1st derivative maximum and the 1st derivative minimum of the peak is proportional to the FWHM, as mentioned in the Appendix. For the quantitative amount of OH content in the deposited SiO_x films, we used two characteristic values from the FT-IR spectra. One is an FT-IR peak intensity of normalized absorbance around 940 cm^{-1} due to vibration between Si and O of Si–OH bond, as shown later in Fig. 3(a).^{20,23,26} This peak and its intensity are presented as OH1 peak and I_{OH1} , respectively. The other one is an integrated area of normalized absorbance intensity from 3000 – 3700 cm^{-1} , in which O–H vibrations of Si–OH and H_2O appear, as shown later in Fig. 3(b).^{22,24,26}

Table I. Abbreviation list of PDH processes with various process gases and NPDH.

Process gas	TEC + $O_3 + O_2$	$O_3 + O_2$	TEC + O_2	O_2	N_2	NPDH
Process name	P_1	P_2	P_3	P_4	P_5	P_0

This broad peak and its integrated area are presented as OH2 peak and S_{OH2} , respectively.

3. Results

3.1. Deposition temperature dependence

Figure 2 shows the deposition temperature T_d dependences of film thickness (circle) d and refractive index (triangle) n of the films deposited with the NPDH and PDH processes, where two samples were measured for each temperature. The black closed and red open plots represent NPDH and PDH, respectively. As can be seen from this figure, d increases with increasing T_d , but over $T_d = 220$ °C, it has a tendency to saturate with T_d . This can be explained by surface and gas-phase reactions.^{10,27–30} It is also found that the films treated by PDH are a little thicker than the NPDH case at every T_d . This is because, even after stopping the supply of SO vapor from the deposition source, a small amount of SO vapor still remains in the reaction chamber for a while. On the other hand, except for the low T_d of 180 °C, the refractive index n increases with T_d monotonically. This is because the film density increases with T_d due to the enhanced chemical reaction so that the higher film density shows the higher refractive index according to the Lorentz–Lorenz model.^{31,32} Furthermore, it is observed that the PDH process increases n a little, compared with the NPDH case. As mentioned later, the PDH process can reduce a number of OH bonds in the deposited SiO_x films, which makes the films densify. For the larger n of the films deposited at $T_d = 180$ °C, densification might be caused by a small amount of impurities due to insufficient chemical reaction by the reactant gas under an insufficiently high T_d , but the reason is not well understood at present.

Figures 3(a) and 3(b) show typical FT-IR spectra of the SiO_x films deposited at 190 °C (solid lines) and 220 °C (broken lines) for the NPDH (black lines) and PDH (red lines) cases, where the wavenumber ranges of (a) and (b) are 700–1030 and 2800–4000 cm^{-1} , respectively. For a reference, a whole spectrum of an NPHD-treated film at 190 °C is shown in Fig. 3(a) as an inset. The peaks at ~ 800 and 940 cm^{-1} in Fig. 3(a) are identified as absorptions due to the bending of Si–O–Si bond (TO_2) and vibration of Si–OH bond, respectively. The broad peaks in Fig. 3(b) consist of

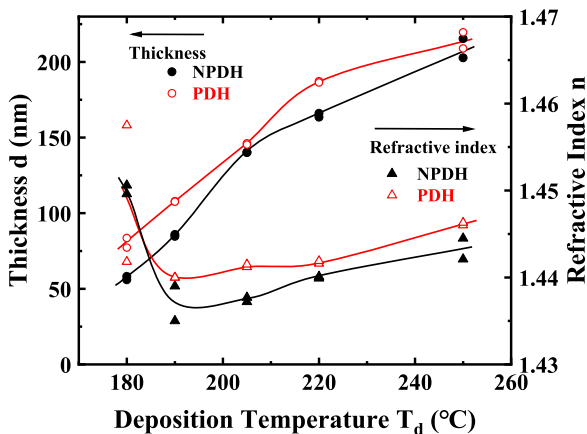


Fig. 2. Deposition temperature T_d dependences of the film thickness (circle) d and refractive index (triangle) n of the films deposited by the NPDH and PDH processes. Data of two samples are plotted for each T_d . Black closed and red open shapes represent NPDH and PDH, respectively.

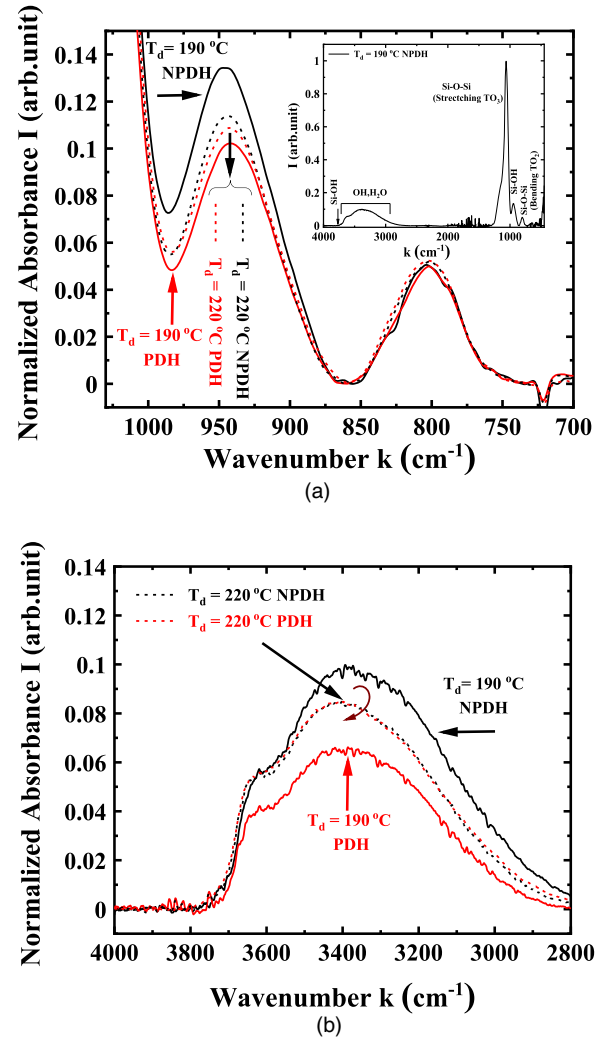


Fig. 3. Typical FT-IR spectra of the films deposited at 190 °C (solid lines) and 220 °C (broken lines) for the NPDH (black lines) and PDH (red lines) cases. Wavenumber ranges of (a) and (b) are 700–1030 and 2800–4000 cm^{-1} , respectively. Inset in Fig. 3(a) shows a whole FT-IR spectrum for the NPDH at 190 °C as a reference.

overlapping vibrations due to O–H of Si–OH and H_2O bond.^{12,20,33} For the $T_d = 190$ °C case, it can be seen from both Figs. 3(a) and 3(b) that the OH1 peak and OH2 broad peak of the NPDH-treated film are decreased by the PDH process. This means that, with the PDH process, OH content including H_2O is reduced due to dehydration reaction of $Si-OH + Si-OH \rightarrow Si-O-Si + H_2O \uparrow$ and evaporation of H_2O . In contrast, for the 220 °C case, the 940 cm^{-1} peak decreases a little from the NPDH to the PDH, and the OH2 broad peak for the NPDH is almost the same as that for the PDH. This means that, for the $T_d = 220$ °C case, the number of OH bonds is hardly changed by the PDH process, which will be discussed in more detail later.

Figure 4 shows the dependences of S_{OH2} (circles) and I_{OH1} (triangles) on deposition temperature T_d , where the black closed and red open shapes indicate the NPDH and PDH cases, respectively. It can be seen from this result that the S_{OH2} and I_{OH1} for the NPDH case are roughly decreased with increasing T_d , which means that increasing T_d reduces OH content due to the enhanced chemical reaction. However, for the PDH case at $T_d \leq 220$ °C, it is very interesting that both S_{OH2} and I_{OH1} are lower than those at 220 °C, which is the

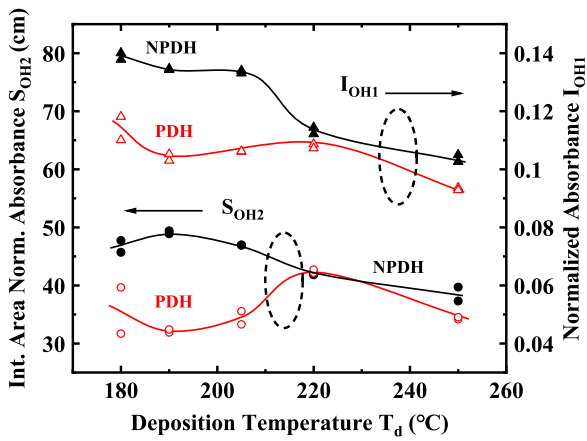


Fig. 4. Dependences of S_{OH2} (circles) and I_{OH1} (triangles) on the deposition temperature T_d . Black and red shapes indicate the NPDH and PDH cases, respectively.

opposite tendency to the NPDH case. This suggests that it be possible to obtain an SiO_x film with lower OH content at lower T_d if the deposition conditions are well controlled. We try to explain this as follows. It can be expected that the structure of a SiO_x film deposited at lower T_d is easily reconstructed due to weaker bond strength between Si and O atoms. In addition, the as-deposited SiO_x films at lower T_d have a greater number of OH bonds compared with the films deposited at higher T_d , as shown in Fig. 4. Therefore, during the PDH process, a substantial number of OH bonds are removed from the as-deposited SiO_x film through an active dehydration reaction between many neighbors of OH bonds, assisted by the wake chemical bonds. This leads to the collapse of numerous microspaces left after the dehydration reaction and to a concomitant rearrangement of the film structure, which makes the film densify, as mentioned previously. This easily reconstructible behavior of SiO_x film is similar to solid phase epitaxial growth of an amorphous Si film on a crystal Si substrate. It has been reported that an amorphous-phase Si film without any crystalline region can easily be crystallized on a crystal Si substrate in solid phase by annealing at a low temperature, e.g. 600 °C (mp of Si: 1410 °C), and an amorphous + crystalline mixed-phase Si film is hardly recovered to a perfect crystal Si with the remaining defects even at much higher temperature.^{34,35} This model is in good agreement with the results of Fig. 2, which show that n of the films is increased due to the PDH process. However, by further increasing T_d to 220 °C, the structure of an as-deposited film becomes harder and contains a smaller amount of OH, both S_{OH2} and I_{OH1} , and after the PDH process are almost the same as those of the NPDH case. Furthermore, by increasing T_d to 250 °C the chemical dehydration reaction becomes more active due to higher thermal energy so that the OH content can be further reduced by the 5 min PDH process from the NPDH case.

Indeed, the structural change of a deposited SiO_x film can be seen by observing the shift of the peak position and shape of the TO_3 mode in the FT-IR spectrum. It is known that wavenumber k_p of a peak position of the TO_3 mode can be approximated by an expression of the form, $k_p = k_0 \sin(\theta/2)$, where k_0 is a constant depending on the mass of the O atom and the force constant between O and Si, and θ is the Si–O–Si

bridging bond angle.^{36,37} Assuming that k_0 is invariant for any deposition condition, a positive or negative shift of k from a standard peak position indicates a positive or negative change in θ from the standard bonding angle. The width of the peak can also be understood in terms of a statistical distribution of θ and summation over narrow angles. Therefore, a change in the k_p and peak form can be regarded as a change of SiO_x film structure. Figure 5 shows the T_d dependences of wavenumbers of the peak position k_p , the 1st derivative maximum k_{pdmax} and the 1st derivative minimum k_{pdmin} of the TO_3 mode peak. Since the TO_3 mode peak is unsymmetric, the k_{pdmin} and k_{pdmax} positions are also unsymmetric with respect to k_p , which means that $(k_{pdmin} - k_p)$ is different to $(k_p - k_{pdmax})$. As can be seen from Fig. 5, at $T_d \leq 205$ °C, the characteristic k values for the PDH case (red lines) are obviously higher than those for the NPDH case (black lines). These results indicates that the film structures were clearly changed by the PDH treatment at $T_d \leq 205$ °C. Consequently, it can also be deduced that the structures of the SiO_x films deposited at $T_d \leq 205$ °C are easily reconstructible compared with that at higher T_d .

By means of the preservation of as-deposited SiO_x films, we investigated the PDH effect on the remaining OH content in the preserved films. The tested samples were SiO_x films deposited at 190 °C and 220 °C, which are the most and the least effective for the reduction of OH content by the PDH process, respectively, as shown in Fig. 4. Figures 6(a) and 6(b) show the typical FT-IR spectra of the SiO_x films deposited at 190 °C and 220 °C, respectively, where the wavenumber range is 2800–4000 cm^{-1} . In each figure, the two films are just as deposited without PDH (NPDH, black) and with PDH (red), and the other two films deposited without PDH (NPDH, blue) and with PDH (green) were preserved for 12 h in dry air.

For the films at $T_d = 190$ °C of Fig. 6(a), the OH content of the NPDH-treated and preserved film (blue) is reduced without heating from that of the as-deposited and NPDH-treated one (black), but with a smaller reduction level than that of the PDH-treated films. This reduction is due to self-dehydration reaction in the film even at RT after deposition since the film structure is easily reconstructible at $T_d = 190$ °C. On the other hand, for the two films treated by the PDH process (red and green lines), the spectral shapes

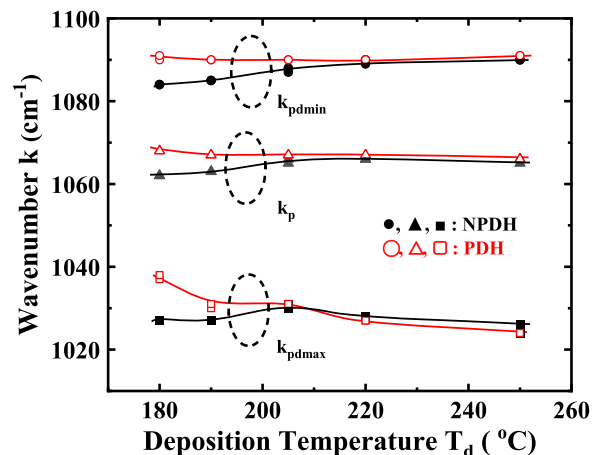


Fig. 5. Deposition temperature T_d dependences of the wavenumbers of the peak position k_p , the 1st derivative maximum k_{pdmax} and the 1st derivative minimum k_{pdmin} of the TO_3 mode peak.

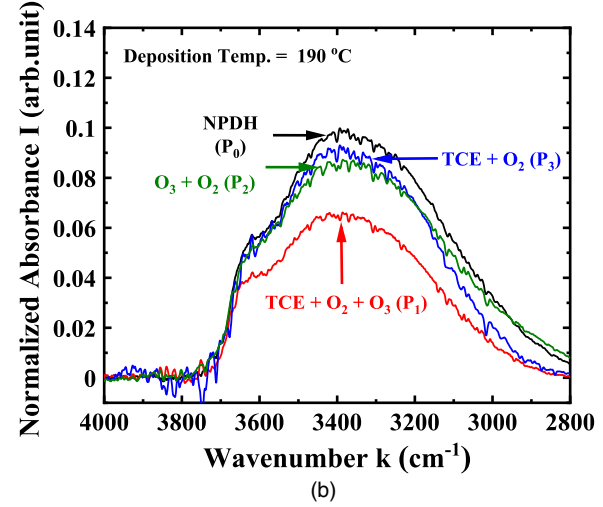
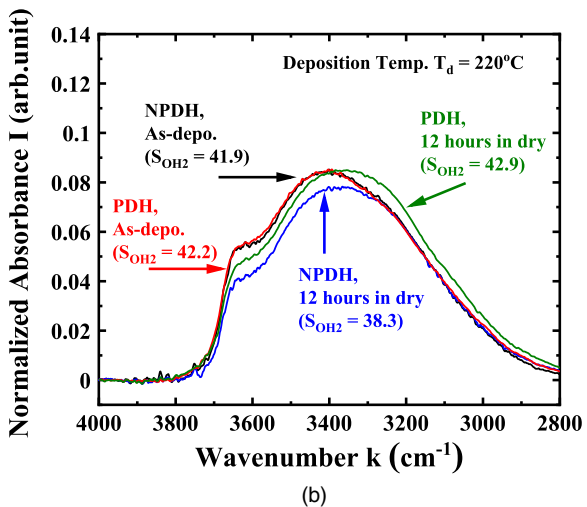
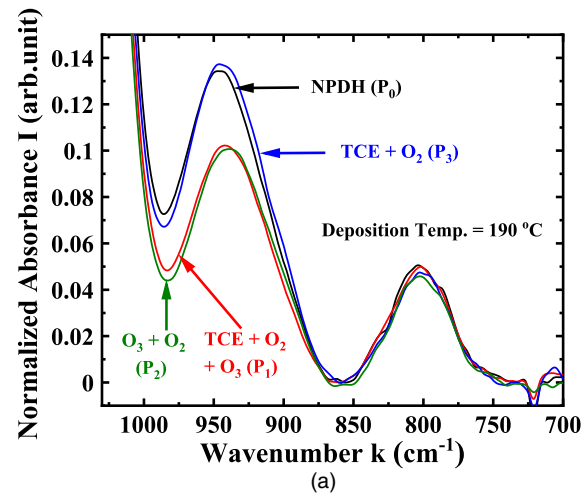
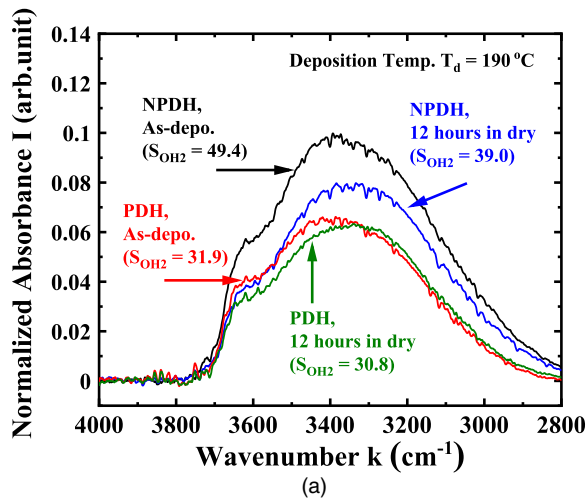


Fig. 6. Typical FT-IR spectra of the SiO_x films deposited at (a) 190 °C and (b) 220 °C in the wavenumber range of 2800–4000 cm^{-1} . Black and red lines represent only as-deposited films with the NPdH and PDH processes, respectively. Blue and green lines represent the preserved films treated by the NPdH and PDH processes, respectively.

Fig. 7. Typical FT-IR spectra of the SiO_x films PDH-treated at 190 °C with the various conditions of the process gas. Wavenumber ranges of (a) and (b) are 700–1030 and 2800–4000 cm^{-1} , respectively. Process gas conditions are P_1 (red line), P_2 (green line) and P_3 (blue line). As a reference, P_0 (black line) of NPdH is shown.

are almost the same, although a small difference can be seen between them in the higher wavenumber range of 3400–3700 cm^{-1} . This means that the PDH-treated SiO_x films are more stable than the ones without the PDH process. In contrast, for the 220 °C-deposition case of Fig. 6(b), the difference in spectral shape is not as large as that in the 190 °C case of Fig. 6(a) regardless of preservation and the PDH process. However, every S_{OH_2} (38 ~ 43) at 220 °C is larger than those (30 ~ 32) of the PDH case at 190 °C, as shown in Fig. 6(b). This means that the PDH process at lower $T_d = 190$ °C is useful and effective not only for reduction of OH content, but also suppression of increment of OH content in preservation. In addition, it can be considered from this result that the structure-changed film due to the PDH process is relatively denser so that moisture or the source of OH bonds might hardly be diffused into the film.

3.2. Dependence on process gas in PDH

Figures 7(a) and 7(b) show typical FT-IR spectra of the SiO_x films deposited and PDH-treated at 190 °C with the various conditions of a process gas, where the wavenumber ranges of (a) and (b) are 700–1030 and 2800–4000 cm^{-1} , respectively. Among the five kinds of PDH processes, P_1 (red line), P_2

(green line) and P_3 (blue line) are selected. In addition, spectra of P_0 (black line) are shown as a reference. From Fig. 7(a), it can be clearly seen that the OH1 peaks for P_1 and P_2 are almost the same, and that those for P_3 and P_0 are also almost the same but much higher than the former ones. On the other hand, in Fig. 7(b), the tendency of normalized absorbance I is a little different to that of Fig. 7(a). While I of P_0 and P_3 [$I(P_0)$ and $I(P_3)$] are almost the same as in Fig. 7(a), $I(P_1)$ is much lower than $I(P_2)$ in Fig. 7(b), which is obviously different to the Fig. 7(a) case of $I(P_1) \approx I(P_2)$.

A comparison of S_{OH_2} and I_{OH_1} in the respective PDH processes is shown as a histogram in Fig. 8 with the NPdH case as a reference, where the light blue and the hatched red bars indicate S_{OH_2} and I_{OH_1} , respectively. For each process gas condition, the bar height is the average of the two samples' data, and the difference between them is presented as a short line or error bar. It can be clearly seen that the process gas of P_1 is the most effective for the reduction of OH content due to the lowest S_{OH_2} and much lower I_{OH_1} . The P_2 process gas is also effective for the lowest I_{OH_1} , but it is not as good due to the relatively high S_{OH_2} compared with that of P_1 . From the viewpoint of I_{OH_1} attributed to vibration between Si and OH (Si–OH), it can be considered that O_3

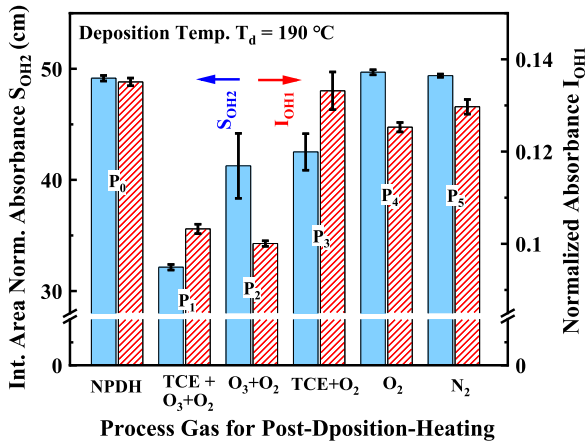


Fig. 8. Comparison of S_{OH2} (light blue) and I_{OH1} (hatched red) in the respective PDH processes with the NPDH case as a reference. For each bar, the average data of two samples are shown and the differences between them are presented as short lines or error bars.

plays a very important role in the reduction of OH bonds since the I_{OH1} of P_1 and P_2 are much smaller than those of the other processes including P_0 . This is probably due to the fact that O_3 assists the dehydration reaction of $Si-OH + Si-OH \rightarrow Si-O-Si + H_2O$, where O_3 acts as a catalyst. The dehydration in P_2 also leads to structural change and densification of SiO_x films such as P_1 , as shown previously. Table II shows the characteristic wavenumbers in a peak of the TO_3 mode for respective P_i processes such as those in Fig. 5. As can be seen, k_p , k_{pdmin} and k_{pdmax} in P_2 as well as P_1 are significantly larger than those of the other processes.

Although it seems that the data of the other processes of P_3 (TCE + O_2), P_4 (O_2) and P_5 (N_2) are roughly similar to those of P_0 (NPDH), a few interesting and curious points can be found when carefully comparing all the data. For example, I_{OH1} of P_2 is much smaller than that of P_3 but their S_{OH2} are almost the same. These discrepancies will be discussed in the next section.

4. Discussion

It can be seen from Fig. 4 that the S_{OH2} behavior is almost similar to I_{OH1} probably because the signal source for both is the Si-OH bond, i.e. S_{OH2} is due to O-H vibration of Si-OH, and I_{OH1} is due to Si-OH vibration. Figure 9 shows the relationship between S_{OH2} and I_{OH1} in this study. In this figure, the black closed and red open circles represent the data for the NPDH- and PDH-treated SiO_x films, respectively. The data are used in Fig. 4, and the blue open triangles represent the films treated by the P_i processes with various gases, whose data are used in Fig. 8 except for P_0 and P_1 . The black broken and red one-point-broken linear lines indicate the roughly proportional relationship between S_{OH2} and I_{OH1} , where the two lines pass through the origin, which is shown

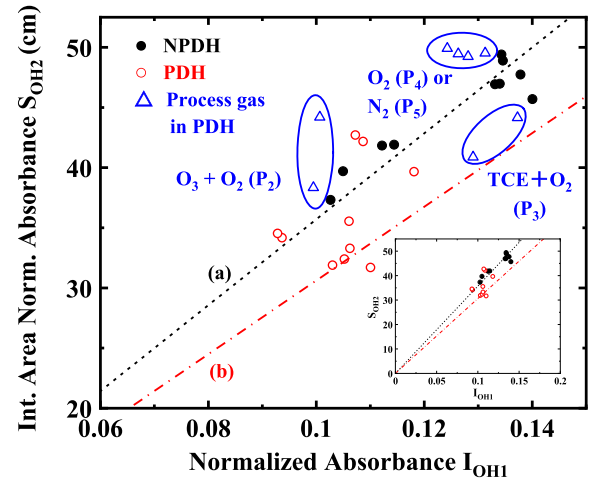


Fig. 9. Relationship between S_{OH2} and I_{OH1} for the NPDH- (black closed circle) and the normal PDH- (red open circle) treated SiO_x films shown in Fig. 3, and for the PDH-treated films with the various process gases P_i (blue open triangle) shown in Fig. 8 except for P_0 and P_1 . Black broken (a) and red one-point-broken (b) linear lines represent roughly proportional relations between S_{OH2} and I_{OH1} , i.e. $S_{OH2} \approx C \cdot I_{OH1}$. C of (a) is larger than that of (b) due to a larger amount of H_2O adsorption on an SiO_x film. Details are mentioned in Sect. 4. Discussion.

in the inset. Thus, the relationship can be expressed as,

$$S_{OH2} \approx C \cdot I_{OH1}, \quad (2)$$

where C is a proportional constant. The black line labeled (a) mainly corresponds to the NPDH data, and the red one labeled (b) mainly to the P_1 data with the lower S_{OH2} . In this case, C for the NPDH and PDH are $C_a = 357$ and $C_b = 306$, respectively. Here, we should note that the measured I_{OH1} is larger, within $\sim 20\%$ of a true I_{OH1} of the OH1 peak because the measured one is overlapped with a small tail or shoulder of the TO_3 mode peak on the lower k side, as shown in Fig. 3(a). However, this overestimation is not an essential issue in physics because it just brings a small error or fluctuation to the proportional constant “ C ”, which are somewhat comparable to the scattered data of the NPDH and PDH cases. Later, we will discuss constant “ C ” more deeply.

Figure 10 shows a typical FT-IR spectrum in the wavenumber range of $2800-4000 \text{ cm}^{-1}$ with schematic pictures of four possible forms of the silanol (Si-OH) group.^{21,33} It is well known that low-temperature deposited SiO_x films contain numerous OH bonds of the silanol group and an amount of water or moisture H_2O .^(3-5,8,12,14,15) Therefore, the silanol groups are perturbed by the H bond action (“- - -”) as in the schematic picture in Fig. 10. Type (a) is an isolated silanol free of H bond, and its O-H stretching mode is responsible for a distinct sharp band at $\sim 3740 \text{ cm}^{-1}$. (b) is a silanol perturbed at the O atom, (c) is at the H atom, and (d) is at both atoms. In (c) and (d), H bonds are formed between

Table II. Wavenumbers (cm^{-1}) at the peak position k_p , the 1st derivative minimum k_{pdmin} , the 1st derivative maximum k_{pdmax} of the TO_3 mode peak for each PDH process. As a reference, the NPDH data are shown. The values are averages of two samples under the same process gas condition.

Gas process	TEC + O_3 + O_2 P_1	O_3 + O_2 P_2	TEC + O_2 P_3	O_2 P_4	N_2 P_5	NPDH P_0
k_{pdmin}	1090	1090	1086	1086	1086	1085
k_p	1067	1067	1064	1064	1064	1063
k_{pdmax}	1031	1033	1030	1029	1028	1027

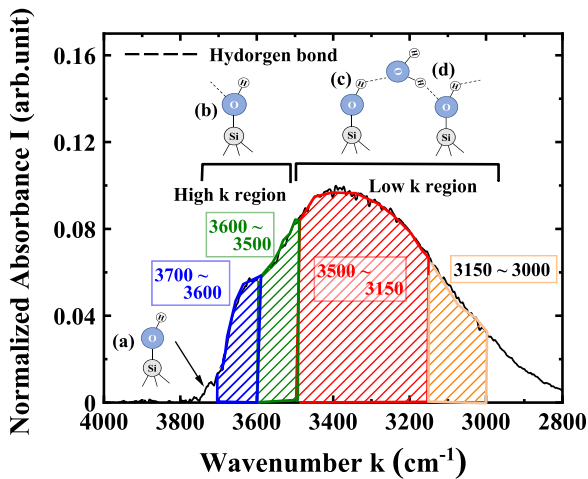


Fig. 10. Typical FT-IR spectrum in the wavenumber range of 2800–4000 cm^{-1} with schematic pictures of four possible forms of the silanol (Si–OH) group. Range of wavenumber k is divided into the four regions according to the degree of affect of H bond on silanol.

silanols and one H_2O molecule. Since H bond affects silanol more strongly, absorption wavenumber k is shifted lower. In other words, when the H bond further weakens the atomic bond strength of O–H in silanol, wavenumber k is further lowered. Here, we divide the range of measurement wavenumber k into four regions, 3700–3600, 3600–3500, 3500–3150, and 3150–3000 cm^{-1} . Figure 11 shows the relationship between the four divided k regions and the ratios in S_{OH_2} of PDH/NHP as a function of the deposition temperature T_d , where the data for 180, 190, 205, 220, and 250 $^\circ\text{C}$ are indicated by black triangle, red circle, blue square, green diamond and pink star shapes, respectively. Each data plot is an average of two samples under the same condition. A lower ratio means a larger reduction in OH content by the PDH process. It can be seen from this figure that the PDH effect on the reduction of S_{OH_2} is stronger in the lower k region at any T_d except for $T_d = 220^\circ\text{C}$. The exception of 220 $^\circ\text{C}$ can be expected based on the results of Fig. 4. Consequently, the

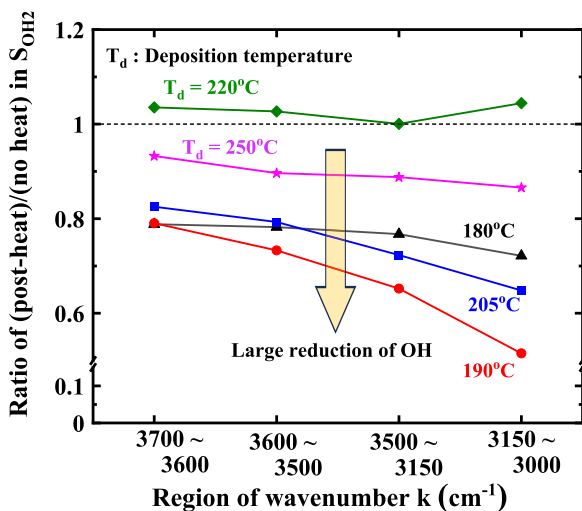


Fig. 11. Relationship between the four divided k regions and the ratios in S_{OH_2} of PDH/NPDH as a function of deposition temperature T_d . Data for 180, 190, 205, 220, and 250 $^\circ\text{C}$ are indicated by black triangle, red circle, blue square, green diamond and pink star shapes, respectively. Each data plot is an average of two samples under the same conditions.

dehydration reaction between OH bonds is further promoted by the stronger effect of the H bond so that Si–OH bonds of the silanol group vanish more easily.

Based on the above discussion, we will further discuss a few questions raised by Fig. 8. Question 1 (Q1): why is the S_{OH_2} of P_2 relatively higher despite its lowest I_{OH_1} ? Q2: why is the I_{OH_1} of P_3 much larger than that of P_2 , although both S_{OH_2} are nearly equal? Q3: why are the error bars of P_2 and P_3 larger compared with the other ones? Finally, Q4: why are the S_{OH_2} of $P_4(\text{O}_2)$ and $P_5(\text{N}_2)$ still higher after the PDH process while their I_{OH_1} are slightly reduced? It is hard to consider that these questions come from faults in measurement and deposition because they have good reproducibility. In order to gain some insight into the answers to these questions, we take the difference in FT-IR spectrum between the P_i processes, as shown in Fig. 12, where the black, blue, and red lines represent the FT-IR spectra of $(P_0 - P_1)$, $(P_2 - P_1)$ and the $(P_2 - P_3)$, respectively. It can be seen from this figure that $(P_0 - P_1)$ is larger as a whole, compared to $(P_2 - P_1)$ and $(P_2 - P_3)$. In addition, the shape of the blue $(P_2 - P_1)$ is round and broad, whereas that of the red $(P_2 - P_3)$, by contrast, is wavy with negative and positive split regions. As shown in Figs. 10 and 11, the H bond effect on silanol is stronger in the lower region of k , which is roughly related to the number of OH bonds and H_2O . Furthermore, H_2O or moisture comes from not only the deposition reaction, but also from adsorption on the surface of SiO_x films through the PDH process and the deposited films being exposed to air.

Taking the above insight and the results of Fig. 12 into account, we try to answer the aforementioned questions Q1 to Q4 as follows. If the amount of H_2O adsorption is assumed to depend on number of Si–OH bonds or I_{OH_1} , the proportional constant “C” of Eq. 2 is caused by O–H vibrations of not only Si–OH, but also H_2O , as shown in Fig. 13. Thus, we can express C as $C = C_{\text{Si-OH}} + C_{\text{H}_2\text{O}}$, where $C_{\text{Si-OH}}$ and $C_{\text{H}_2\text{O}}$ are attributed to Si–OH and H_2O , respectively. Therefore, the difference in I of $(P_2 - P_1)$ in Fig. 12 may be due to the difference in the amount of adsorbed H_2O on the sample or $C_{\text{H}_2\text{O}}$. This can be the answer to Q1. In fact, the plots of P_2 in Fig. 9 are above the broken (a) line. Likewise, we can answer Q2. Since the two P_3 plots are within the two (a) and (b) lines in Fig. 9, the $C_{\text{H}_2\text{O}}$ for P_3 should be smaller than that for P_2 , which means that the ratio amount of adsorbed H_2O and silanol for P_3 , $C_{\text{H}_2\text{O}}/C_{\text{Si-OH}}$, is smaller than

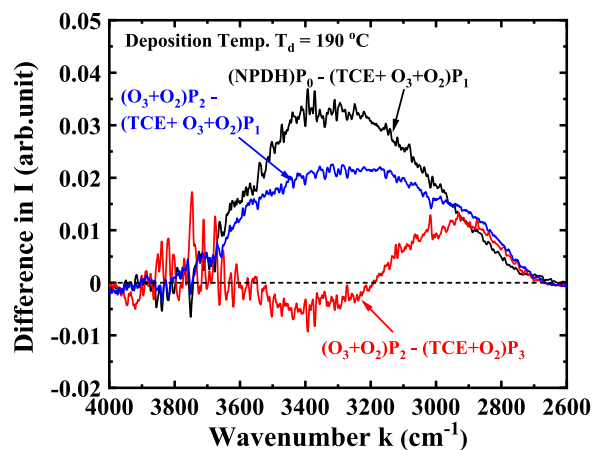


Fig. 12. Difference in FT-IR spectra of $(P_0 - P_1)$ (black), $(P_2 - P_1)$ (blue) and $(P_2 - P_3)$ (red). P_i is a PDH process abbreviation with one kind of process gas and the detail is given in Table I.

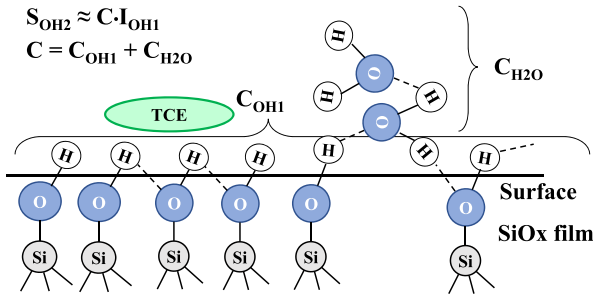


Fig. 13. Schematic model to explain the relationship between S_{OH2} and I_{OH1} shown in Fig. 9. S_{OH2} can be expressed as $S_{OH2} \approx C \cdot I_{OH1}$, where C is a proportional constant and is attributed to two factors of C_{Si-OH} and C_{H2O} , where C_{Si-OH} and C_{H2O} originate from Si-OH and H₂O, respectively.

that for P₂. Furthermore, we can explain why the H₂O adsorption constant C_{H2O} for P₂ is larger than those for P₁ and P₃. As shown in Fig. 13, an amount of hydrophobic TCE, which is a PDH process gas, probably adsorbs and remains on the surface of the deposited SiO_x film in the P₁ and P₃ cases. Thus, the adsorption of hydrophilic H₂O from the atmosphere may be prevented on the TCE-adsorbed surface. In contrast, H₂O adsorption in the P₂ case can easily occur on a surface almost without TCE. This small amount of TCE on the surface results from there being no TCE supply and the removal of TCE that remains on the surface due to chemically reactive O₃ during the PDH process. The explanation with TCE adsorption can also be applied to an answer for Q3 in respect of the relatively larger error bars in S_{OH2} of the P₂ and P₃ cases. This is because the degree or amount of TCE adsorption on the surface of a deposited oxide film is somehow uncertain and difficult to strictly control. In addition, covering the film surface with TCE might influence the I_{OH1} value of P₃ since the error bar of I_{OH1} is large. Finally, we discuss Q4, i.e., the reason why the I_{OH1} of P₄ and P₅ are a little smaller than that of the NPDH while the I_{OH1} of P₃, in which only TCE is added to P₄, is at the same level as the NPDH. The small reduction in I_{OH1} for P₄ and P₅ can be explained by the so-called annealing effect through the 5 min PDH process. However, for the I_{OH1} of P₃, we still do not have a clear answer, although there is the possibility that TCE might somehow prevent the annealing effect.

We have discussed the Q1 to Q4 questions, as mentioned above, and explained the answers. However, some unanswered questions still remain because we do not know enough about the detailed mechanisms of SiO_x film growth at present. Consequently, further discussion and investigation is necessary.

5. Conclusion

In this study, we investigated the PDH effect on OH content in the SiO_x films deposited by APCVD using the deposition source of SO with the reactive gas of O₃ and TCE vapor at the temperature T_d of 180 °C–250 °C. The PDH process is performed in situ for 5 min without any supply of SO in the deposition chamber just after film deposition, where the heating temperature is the same as T_d . While OH content in the films without the PDH process or with the NPDH process decreased with increasing T_d due to thermal-energy-enhanced chemical reaction, those with the PDH process decrease with decreasing T_d from 220 °C. At $T_d = 190$ °C, the minimum OH content in the SiO_x film can be obtained. This PDH effect on

OH reduction can be considered due to the easily reconstructible structure of SiO_x films deposited at lower T_d . This reconstructible structure probably results from weaker bond strength between Si and O atoms and is promoted by the large number of OH bonds in SiO_x film deposited at lower T_d , where a substantial amount of the OH bonds are removed by dehydration reaction in the PDH process. This is a curious point for the low-temperature deposition of SiO_x film because lower OH content can be obtained at lower temperature in the case of limited $T_d \leq 200$ °C. Furthermore, we found one key process gas for the reduction of OH content in the PDH process. This is O₃, which acts as a catalyst for the reduction of OH bonds. For TCE, it plays the role of suppression of H₂O adsorption on an as-deposited SiO_x film, in particular, air exposure of a film probably due to its hydrophobic property. However, it may have no effect on the reduction of OH content in deposited SiO_x films after deposition.

Acknowledgment

This research is partially supported by JSPS KAKENHI, Grant No. JS21K04649.

Appendix

Assuming that the peak form is a Gaussian curve, the peak intensity I as a function of k is expressed by,

$$I(k) = \exp\left(-\frac{k^2}{2W^2}\right), \text{ where } I(0) = 1. \quad (\text{A-1})$$

Then, the 1st derivative and the 2nd derivative of Eq. (A-1) are calculated as,

$$I'(k) = -\frac{k}{W^2} \exp\left(-\frac{k^2}{2W^2}\right), \quad (\text{A-2})$$

and

$$I''(k) = \frac{1}{W^2} \left(\frac{k^2 - W^2}{W^2}\right) \exp\left(-\frac{k^2}{2W^2}\right). \quad (\text{A-3})$$

Therefore, k values at the negative minimum of $I'(k)$, k_{dmin} , and the positive maximum, k_{dmax} , are W and $-W$, respectively. Because FWHM of $I(k)$ is calculated to be $2\sqrt{\ln(2)}W$, the FWHM is proportional to $k_{dmin} - k_{dmax} = 2W$.

- 1) S. Higashi, D. Abe, S. Inoue, and T. Shimoda, *Jpn. J. Appl. Phys.* **40**, 4171 (2001).
- 2) M. M. Moslehi, R. A. Chapman, M. Wong, A. Paranjpe, H. N. Najm, J. Kuehne, R. L. Yeakley, and C. J. Davis, *IEEE Trans. Electron Devices* **39**, 4 (1992).
- 3) T. Kawahara, A. Yuuki, and Y. Matsui, *Jpn. J. Appl. Phys.* **31**, 2925 (1992).
- 4) N. Hirashita, S. Tokitoh, and H. Uchida, *Jpn. J. Appl. Phys.* **32**, 1787 (1993).
- 5) A. M. Mahajan, L. S. Patil, J. P. Bange, and D. K. Gautam, *Vacuum* **79**, 194 (2005).
- 6) G. Mannino, R. Ruggeri, A. Alberti, V. Privitera, G. Fortunato, and L. Maiolo, *Appl. Phys. Express* **5**, 021103 (2012).
- 7) T. Toriyabe, K. Nishioka, and S. Horita, Proc. 13th Int. Display Workshops (IDW'06), 2006, p. 719.
- 8) S. Horita, K. Toriyabe, and K. Nishioka, *Jpn. J. Appl. Phys.* **48**, 035502 (2009).
- 9) H. Nakashima, K. Omae, T. Takebayashi, C. Ishizuka, and T. Uemura, *J. Occup. Health* **40**, 270 (1998).
- 10) S. Horita and P. Jain, *Jpn. J. Appl. Phys.* **56**, 088003 (2017).
- 11) P. Jain and S. Horita, Proc. 21st Int. Workshop Active-Matrix Flatpanel Displays and Devices (AM-FPD), 2017, p. 285.
- 12) S. Horita and P. Jain, *Jpn. J. Appl. Phys.* **57**, 03DA02 (2018).

- 13) J. McMurry, *Fundamentals of Organic Chemistry* (Brooks/Cole, Belmont, CA, 2011) 7th ed., p. 339.
- 14) M. Matsuura, Y. Hayashide, H. Kotani, and H. Abe, *Jpn. J. Appl. Phys.* **30**, 1530 (1991).
- 15) Y. Nishi, T. Funai, H. Izawa, T. Fujimoto, H. Morimoto, and M. Ishii, *Jpn. J. Appl. Phys.* **31**, 4570 (1992).
- 16) T. Ito, T. Matumoto, and K. Nishioka, *Surf. Coat. Technol.* **215**, 447 (2013).
- 17) S. S. Kim, D. J. Stephens, G. Lucovsky, G. G. Fountain, and R. J. Markunas, *J. Vac. Sci. Technol. A* **8**, 2039 (1990).
- 18) L. C. D. Goncalves, C. E. Viana, J. C. Santos, and N. I. Morimoto, *Surf. Coat. Technol.* **180–181**, 275 (2004).
- 19) S. Horita and D. Pu, Abstr. 9th Int. Symp. Organic and Inorganic Electronic Materials and Related Nanotechnologies, 2023, p. 283, EM-NANO 2023.
- 20) J. A. Theil, D. V. Tsu, M. W. Watkins, S. S. Kim, and G. Lucovsky, *J. Vac. Sci. Technol. A* **8**, 1374 (1990).
- 21) H. Rinnert and M. Vergnat, *J. Non-Cryst. Solids* **320**, 64 (2003).
- 22) P. Lange, U. Schnakenberg, S. Ullerich, and H.-J. Schliwinski, *J. Appl. Phys.* **68**, 3532 (1990).
- 23) A. Barranco, F. Yubero, J. Cotrino, J. P. Espinós, J. Benítez, T. C. Rojas, J. Allain, T. Girardeau, J. P. Rivière, and A. R. González-Elipe, *Thin Solid Films* **396**, 9 (2001).
- 24) P. Innocenzi, P. Falcaro, D. Grosso, and F. Babonneau, *J. Phys. Chem. B* **107**, 4711 (2003).
- 25) A. Savitzky and M. J. E. Golay, *Anal. Chem.* **36**, 1627 (1964).
- 26) R. M. Almeida and C. G. Pantano, *J. Appl. Phys.* **68**, 4225 (1990).
- 27) K. Fujino, Y. Nishimoto, N. Tokumasu, and K. Maeda, *J. Electrochem. Soc.* **137**, 2883 (1990).
- 28) Y. Ikeda, Y. Numasawa, and M. Sakamoto, *J. Electron. Mater.* **19**, 45 (1990).
- 29) E. J. Kim and W. N. Will, *J. Cryst. Growth* **140**, 315 (1994).
- 30) M. Ouyang, C. Yuan, R. J. Muisener, A. Boulares, and J. T. Koberstein, *Chem. Mater.* **12**, 1591 (2000).
- 31) L. Bányai and P. Gartner, *Phys. Rev. B* **29**, 728 (1984).
- 32) K. E. Oughstun and N. A. Cartwright, *Opt. Express* **11**, 1541 (2003).
- 33) A. Fidalgo and L. M. Ilharco, *J. Non-Cryst. Solids* **283**, 144 (2001).
- 34) M. Miyao, N. Yoshihiro, T. Tokuyama, and T. Mitsuishi, *J. Appl. Phys.* **50**, 223 (1979).
- 35) H. Ishiwara and S. Horita, *Jpn. J. Appl. Phys.* **24**, 568 (1985).
- 36) G. Lucovsky, M. J. Manitini, J. K. Srivastava, and E. A. Irene, *J. Vac. Sci. Technol. B* **5**, 530 (1987).
- 37) J. T. Fitch, G. Lucovsky, E. Kobeda, and E. A. Irene, *J. Vac. Sci. Technol. B* **7**, 153 (1989).